



*drones*



Article

---

# Seismic Data Acquisition Utilizing a Group of UAVs

---

Artem Timoshenko, Grigoriy Yashin, Valerii Serpiva, Rustam Hamadov, Dmitry Fedotov, Mariia Kartashova and Pavel Golikov

## Special Issue

Resilient Networking and Task Allocation for Drone Swarms

Edited by

Prof. Dr. Jingjing Wang and Dr. Yibo Zhang



<https://doi.org/10.3390/drones9030156>

## Article

# Seismic Data Acquisition Utilizing a Group of UAVs

Artem Timoshenko <sup>1,\*</sup>, Grigoriy Yashin <sup>1</sup>, Valerii Serpiva <sup>1</sup>, Rustam Hamadov <sup>1</sup>, Dmitry Fedotov <sup>1</sup>,  
Mariia Kartashova <sup>1</sup> and Pavel Golikov <sup>2</sup>

<sup>1</sup> Aramco Research Center—Moscow, Aramco Innovations LLC, 117105 Moscow, Russia;  
grigoriy.yashin@aramcoinnovations.com (G.Y.); valerii.serpiva@aramcoinnovations.com (V.S.);  
rustam.hamadov@aramcoinnovations.com (R.H.); dmitry.fedotov@aramcoinnovations.com (D.F.);  
maria.kartashova@aramcoinnovations.com (M.K.)

<sup>2</sup> EXPEC Advanced Research Center, Dhahran 31311, Saudi Arabia; pavel.golikov@aramco.com

\* Correspondence: artem.timoshenko@aramcoinnovations.com

**Abstract:** Seismic exploration in hard-to-reach hazardous environments like deserts is a very expensive and time-consuming process that involves a lot of human resources and equipment. These difficulties can be overcome with the implementation of robots, providing flexible mission design, safe operation, and high precision data acquisition. This work presents an autonomous robotic system to assist seismic crews in advanced data acquisition for near-surface characterization, shallow cavity detection, and acquisition grid infill. The developed system consists of a swarm control station and a swarm of unmanned aerial vehicles (UAVs) equipped with seismic sensors. The architecture of the swarm control station, its individual blocks, features of UAV exploitation for seismic data acquisition tasks, hardware and software tool limitations are considered. Algorithms for planning UAV swarm flight paths, their comparison and trajectory examples are presented. Experiments utilizing 9 and 16 UAVs to record 171 and 144 target points, respectively, in harsh desert conditions are described. The results demonstrate the feasibility of the proposed system for seismic data acquisition. The developed robotic system offers flexibility in seismic survey design and planning, enabling efficient coverage of vast areas and facilitating comprehensive data acquisition, which enhances the accuracy and resolution of subsurface seismic imaging.



Academic Editors: Jingjing Wang and  
Yibo Zhang

Received: 20 January 2025

Revised: 15 February 2025

Accepted: 17 February 2025

Published: 20 February 2025

**Citation:** Timoshenko, A.; Yashin, G.; Serpiva, V.; Hamadov, R.; Fedotov, D.; Kartashova, M.; Golikov, P. Seismic Data Acquisition Utilizing a Group of UAVs. *Drones* **2025**, *9*, 156. <https://doi.org/10.3390/drones9030156>

**Copyright:** © 2025 by the authors. Licensee MDPI, Basel, Switzerland. This article is an open access article distributed under the terms and conditions of the Creative Commons Attribution (CC BY) license (<https://creativecommons.org/licenses/by/4.0/>).

## 1. Introduction

Seismic exploration is one of the methods widely used for prospecting mineral and hydrocarbon deposits and for engineering surveys of ground surfaces before or after the construction of structures. This method involves the exploitation of a powerful source (hydraulic shaker, accelerated weight drop, electromagnetic vibrator, etc.) to generate seismic waves and then register their reflected component by the receivers placed on the ground surface. Extreme weather conditions, lack of roads and infrastructure significantly complicate seismic exploration in desert and mountainous regions [1]. The next challenge appears at the initial stage of oil well drilling, where shallow karst formations pose significant danger, e.g., in well-pad construction [2]. The intricate nature and relatively small scale of shallow subsurface anomalies necessitate the design of a denser geophysical survey. Automation of the process of collecting seismic data using robotic systems is one of the most promising approaches not only for solving current problems, but also helps to accelerate the introduction of innovations in such a conservative area. Over the past

few decades, concepts of autonomous seismic exploration using robotic devices in various environments have been formulated [3]. Autonomous underwater vehicles (AUVs) have been developed for seafloor seismic acquisition, terrestrial robots for land seismic exploration and unmanned aerial vehicle (UAVs) for sensor deployment. The greatest variety of solutions is presented on the basis of UAVs, which are the most mobile units for performing various tasks [4]. Since 2005, active research and testing of various types of UAVs for conducting magnetic surveys has been ongoing [5]. This trend has resulted in several types of commercially available UAVs. Another popular application of UAVs is mapping in the context of geohazards [6] associated with mass earth movements [7], volcanology [8], flooding events [9] and earthquakes [10]. UAVs equipped with different cameras are used to obtain 3D point clouds or orthophotos with post-processing techniques using photogrammetry software and georeferencing methods. An example of this is the usage of UAVs for on-demand area scouting to aid near-surface geoscience data acquisition campaigns [11]. This approach provides accurate terrain information to design optimized data acquisition plans with higher efficiency, productivity, and fewer field hours. Also, one of the most promising concepts is the use of UAVs to automate some seismic exploration processes, which has been implemented in several projects with different architectures, as outlined below:

- UAVs with integrated seismic sensors and recorders [12,13];
- UAVs for delivery and dropping of seismic sensors with recorders above the surface [14,15];
- UAVs as a seismic source [16].

In 2017, the deployment of seismic sensors by UAVs proved its effectiveness [15]. A full-scale seismic survey involves the use of a large number of nodes. In the case of dropping a seismic sensor from a UAV to the surface, the UAV can deploy several nodes in one flight. Thus, the limitations depend on the robot's ability to carry a certain number of nodes. On the other hand, this method does not involve validation of successful coupling of the dropped node, or the need for additional means to collect nodes after the survey is completed. The architecture of a UAV with integrated sensors and a seismic recorder (UAV-node) is free from these disadvantages, but requires a large number of robots.

Since 2021, the Autonomous Seismic Acquisition Device (ASAD) has been under development to conduct an autonomous seismic exploration mission for specialized surveying applications such as near-surface characterization, seismic-while-drilling, acquisition infill, passive seismic monitoring, etc. Patent application [17] presents a scalable verified architecture for a robotic system using a swarm of UAVs. Coordination of an exploration mission and the safe flight of the ASAD group (Figure 1) was implemented using the Flight Planning and Control System (FPCS) launched on the Swarm Control Station (SCS). The field tests were performed in desert conditions in Saudi Arabia.

This paper describes the implementation features and technical solutions adopted in the development of a commercial system for an autonomous mission to collect seismic data. The article reveals the architecture of the UAV swarm control system, as well as the adaptation of methods used in robotics to the unique requirements inherent in geophysical exploration of the area. We developed a new robotic system for a practical industrial challenge in the field of seismic exploration automation among the few studies in this area. Our solution has been successfully benchmarked with a traditional seismic data acquisition system in real desert conditions.



**Figure 1.** Group of 20 ASADs on an autonomous mission under the control of FPCS.

## 2. Background and Previous Studies

### 2.1. Land Seismic Data Acquisition

Seismic exploration is a method of detailed investigation of the structure of subsurface layers based on seismic data. The data acquisition is carried out by recording seismic waves reflected by the subsurface layer boundaries using sensors located on the surface. The seismic waves are generated by a seismic source, which can be explosives, seismic vibrators, sledgehammers, etc. [18].

Due to the fact that seismic exploration is one of the most significant methods of geophysical land exploration, relevant equipment is constantly being developed and improved. The number of recording channels is increasing significantly in response to data demands from geophysicists, for example, modern systems include more than 100,000 channels [19]. The usage of a wireless nodal sensor network consisting of MEMS sensors is being considered to facilitate the deployment of large numbers of sensors [20,21]. Recently, a seismic survey was conducted using 166,000 wireless nodes deployed on 4.5 million receiving points (Faster and better subsurface imaging for reservoir optimization, available at [https://read.nxtbook.com/gulf\\_energy\\_information/world\\_oil/june\\_2024/g\\_g\\_otoole\\_stryde\\_.html](https://read.nxtbook.com/gulf_energy_information/world_oil/june_2024/g_g_otoole_stryde_.html) (accessed on 23 September 2024)).

### 2.2. Robotics in Seismic Exploration

There has been growth reported in robotic projects related to seismic exploration. The basic principles and concepts of using robotic systems to automate field processes in seismic data collection in different environments have been formulated [3,22,23]. Among the existing projects, the following groups can be distinguished: AUVs for seafloor seismic acquisition, terrestrial robots for land seismic exploration and UAVs for sensor deployment.

In 2013, an AUV was developed to automate the process of seafloor seismic acquisition and gradually replace bulky equipment that requires a large maintenance crew and expensive delivery methods [24]. Tsingas et al. demonstrated the advantages of the nodal system of seismic recorders, which can be combined with robots to provide the possibility of flexible design of seismic exploration due to the mobility of units. In 2017, 200 AUVs were tested in the Mediterranean Sea and seismic data were recorded underwater on area of  $5.04 \text{ km}^2$  [25].

In 2015, a device for mechanized deployment of seismic sensors was developed. Automator (Automator, available at <https://geophysicaltechnology.com/products/automator/>

(accessed on 23 September 2024)) is based on a trailer with tracks and is able to plant 160 nodes before reloading. This system makes sensor deployment easier, but the task of collecting sensors and loading them into cassettes for the subsequent cycle of sensor placement remains. In 2024, laboratory experiments were conducted on a group of tracked robots equipped with geophones for a distributed subsurface imaging [26]. This development is being carried out for potential application in future planetary missions.

The use of UAVs in the automation of seismic data collection has been implemented in several projects. One of the first projects was an UAV with a built-in seismic sensor and a seismic signal recording device [12]. The bulkiness of the solution affected the vector of project development. The focus was shifted to search for additional solutions. In the second iteration, an UAV capable of carrying several wireless seismic nodes in the dart format [14] was tested. The dart nodes are deployed by dropping them from the UAV over the points where it is planned to record the seismic signal. However, the collection of nodes for downloading the recorded data required another additional robot. An additional experiment was conducted with a legged robot, but this method of movement significantly reduced the speed of data collection. The concept of the UAV-based solution with a built-in sensor and seismic recorder was modified and scaled to flying sensors named ASADs [27]. ASADs can be combined together into a group with a centralized control system to perform joint tasks [13].

### 2.3. Managing a Group of Robots

The above-mentioned projects devoted to AUVs and terrestrial robots involve the usage of a robotic group to ensure maximum efficiency of the proposed solutions, which requires implementation special methods for managing multiple agents. The autonomous control of mobile robots is based on a multilayer system of computing modules that plan and coordinate the trajectory of the robot or robots in a group according to the mission constraints [28,29]. The centralized control system of a group implements some layers on the control device (Master), and the remaining layers on the executing devices (Slaves). One of the main modules is a path planner, which can be implemented on the Master side [30]. This reduces the necessary calculations on the computing modules of the robots by using a more powerful ground station as a Master.

Some methods of path planning for a group of UAVs, such as the A\* graph-based algorithm, artificial potential field (APF) method and their modern modifications, have been considered in reviews and books [29,31]. Graph-based path planning is used in environments cluttered with obstacles. Farid et al. [32] introduces a modified heuristic A\* algorithm with a truncation mechanism to address these challenges. The approach separates motion planning into two steps: finding the shortest path and generating a smooth trajectory. Bentes et al. [33] proposed a dynamic swarm formation approach using APF, extended to 3D environments. It proposes a method to adjust swarm configuration dynamically when avoiding obstacles by combining APF with a global planner like A\*.

Due to the versatility and efficiency of the APF method in UAV trajectory planning, the algorithm continues to be modified to solve various challenges in recent studies. Batinovic et al. [34] showcased APF's real-time obstacle avoidance capabilities using 3D sensors. They introduced a rotation-based component to address local minima, improving trajectory planning and collision avoidance. Huang et al. [35] extended APF's utility by combining it with a random tree algorithm, resulting in the potential field Rapidly exploring Random Tree (PF-RRT).

Trajectory optimization methods applied to path planning are used to refine trajectories in dynamic environments. Ratliff et al. [36] introduced Covariant Hamiltonian Optimization for Motion Planning (CHOMP), which uses covariant gradient techniques to

improve sampled trajectories and optimize higher-order dynamics, making it suitable for standalone motion planning. In autonomous driving, Katerishich et al. [37] developed the Dynamic Neural Field Optimal Motion Planner (DNFOMP), further advancing trajectory optimization by smooth and safe motion planning.

#### 2.4. Challenges

Automation of seismic data collection processes using a group of ASADs can facilitate or even solve the following problems:

- Impact of harsh climatic conditions on crew personnel;
- Routine operations performed by a large number of people;
- Time-consuming exploration preparation and sensor network reconfiguration;
- Impossibility or difficulty of exploring hard-to-reach areas, e.g., mountains and deserts;
- Lack of infrastructure in the exploration area.

### 3. Materials and Methods

The developed autonomous seismic acquisition setup consists of three components: the Swarm Control Station (SCS), a group of ASADs and Hit Recording Module (HRM). An example of the system setup is shown in Figure 2. The whole control system may be divided into four levels as shown in Figure 3:

- User level: graphical user interface (GUI).
- High level (strategic): mission planner.
- Middle level (command): control firmware on on-board computer.
- Low level (executive): executive subsystems of a robot.

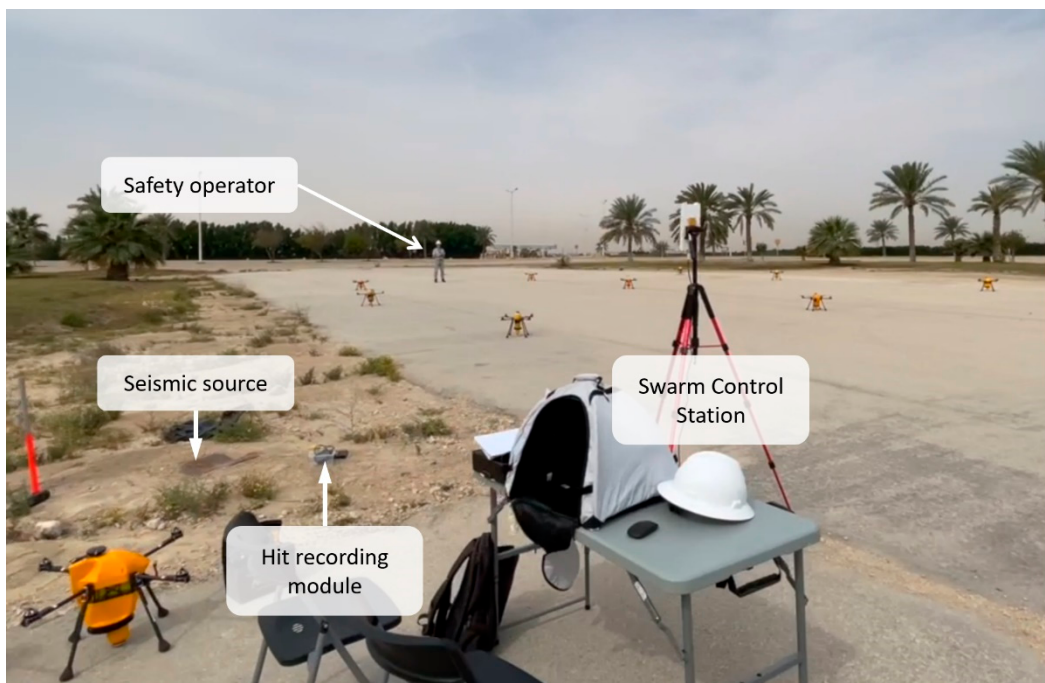


**Figure 2.** Photo of system setup for test with 9 ASADs.

User and high levels are represented by the SCS and the FPCS, while middle and low levels are represented by ASADs themselves and their control firmware.

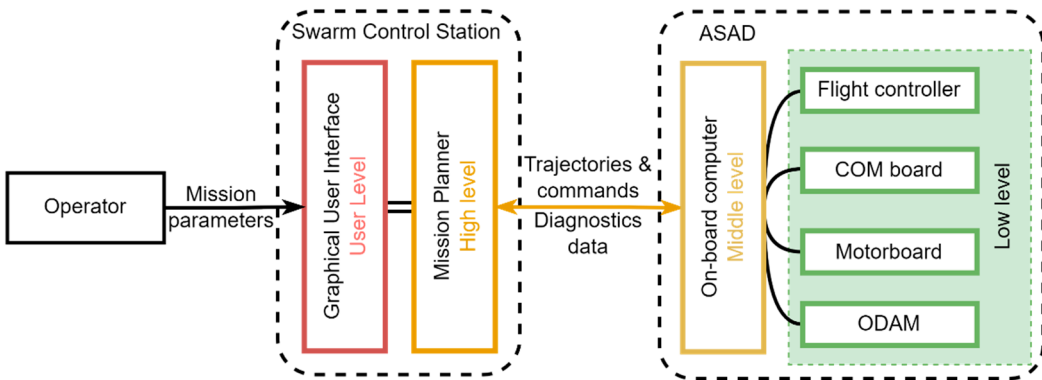


**Figure 3.** System general architecture.

### 3.1. Swarm Control Station

The SCS controls the group of ASADs using a laptop with installed FPCS application. The general scheme of the ASAD system is shown in Figure 3. This system for autonomous geophysical exploration implies the presence of four levels of control.

The device that implements the user and high levels is the Swarm Control Station (SCS). At this stage, the SCS consists of the following three devices:

- A mobile device (laptop or tablet) with a Windows operating system and embedded Wi-Fi module.
- Wi-Fi router to provide large channel capacity and necessary number of connected devices.
- Amplifier and professional antennas to increase the coverage area of the Wi-Fi network (up to 200 m) during field tests.
- A device with long-range radio communication (LoRa) module.

### 3.2. Flight Planning and Control System

The architecture of the FPCS application is presented in Figure 4. The developed application is based on the “tkinter” (Tk interface, available at [docs.python.org](https://docs.python.org) (accessed on 23 September 2024)) Python package and implements the following functions:

- Interaction with user;
- Autonomous mission parameter input;
- Managing the networked group of ASADs;
- Path-planning and flight mission plan generation.

To provide stable and robust connection with multiple ASADs, the multi-thread application architecture with the TCP/IP Server is implemented. The Command Processor and Mission Planner are run on their personal threads to separate message processing and high-performance calculations from the main thread. The TCP Server is run on two threads for processing user commands and to handle incoming connections and allocate a client handler for each connection. Each client handler is run on a separate thread to support several device (ASADs and HRM) connections.

The flight mission plan for a group of ASADs is prepared by four modules: Task Manager, Point Distributor, Path Planner, and Task List Generator. The Task Manager receives the input parameters of the mission from the graphical elements of GUI filled in by the Operator. These parameters include coordinates of target acquisition points, recording time, number of ASADs, their start positions, and mission timings. The Task Manager creates a general sequence of mission tasks and calculates timings of flight to the target position, sensor placement, and data recording. Then, the Point Distributor algorithm, based on the Constrained Hungarian Method for Swarm Drones Assignment

(CHungSDA) [38], distributes target points among UAVs. It provides optimal distribution between the start and target poses for UAV path planning with minimum number of path intersections.

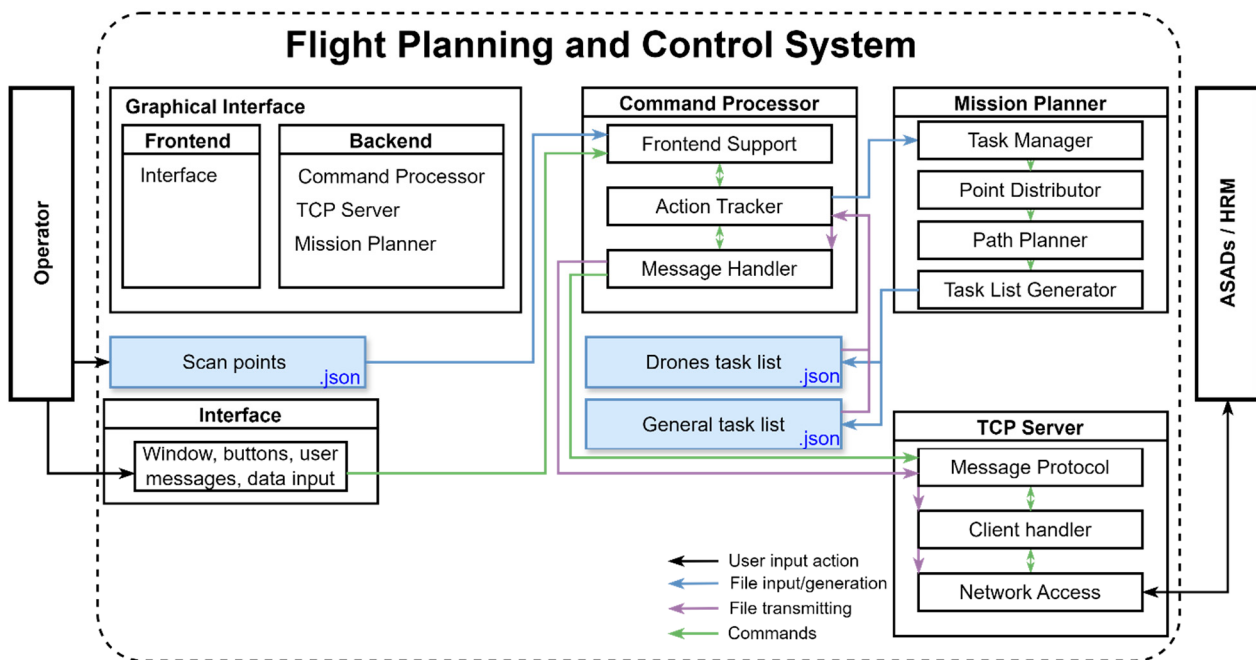


**Figure 4.** FPCS architecture.

Path Planner generates flight paths for UAVs from their origin positions to their target positions based on the A\* search algorithm [39] commonly employed in navigation and pathfinding tasks. This algorithm efficiently explores a graph representing the environment, finding the optimal path from a starting point to a goal while considering heuristic estimates to guide its search. In the concept of autonomous seismic acquisition by UAVs, the target positions for sensor placement are divided into recording areas, each containing a set of points where ASADs should land. Thus, Path Planner prepares three sets of trajectories:

- Trajectories from the origin positions to the first recording area of the seismic exploration zone.
- Trajectories between target data recording points where it must conduct multiple flights through designated recording areas. When there are a large number of target points, several flights of a group of ASADs are required. In this case, the ASADs have the same trajectories for the group flight, and Path Planner duplicates these trajectories. An example for a  $4 \times 4$  group of ASADs is shown in Figure 5.
- Trajectories for return route to the origin positions.

The current ASAD version does not have an integrated communication interface between UAVs in the group, since the Path Planner generates flight paths without the intersection of UAV trajectories.

Finally, Task List Generator converts planned trajectories and tasks into task lists for each ASAD making a schedule for the mission. Each task list includes the ID, mission timetable, task type, coordinates of trajectory points, coordinates of origin position and recording time to perform its assigned tasks during the mission. The task lists are transferred to the ASADs using a communication module that utilizes the TCP server-client protocol through a Wi-Fi network. Also, task lists could be transmitted to the visualization module to check the correctness of the generated trajectories.

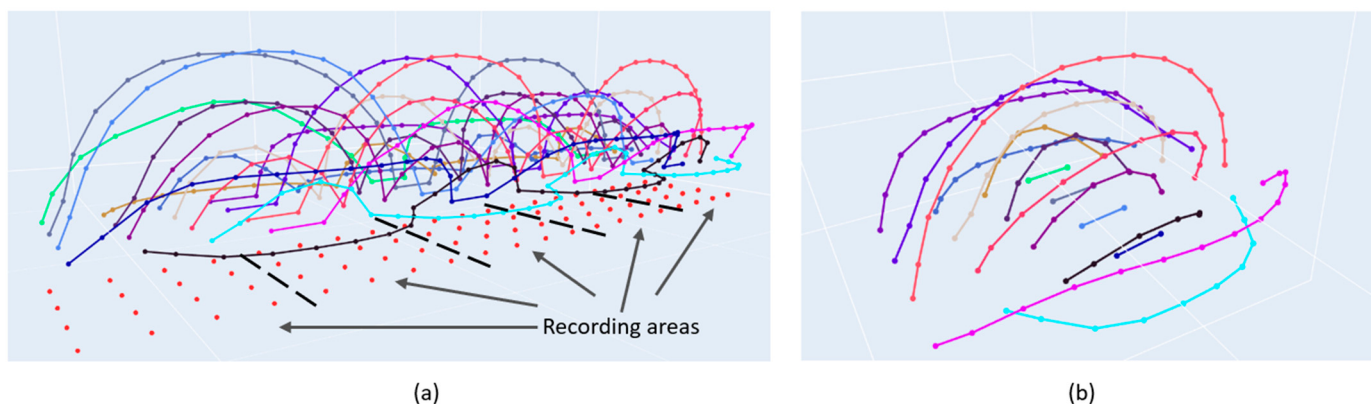


**Figure 5.** Visualization of the generated trajectories for  $4 \times 4$  ASAD formation, where the trajectory of each ASAD is shown in an individual color and the red dots are target points: (a) trajectories for whole seismic exploration zone; (b) trajectories for one recording area.

An example of the mission schedule for 9 ASADs with data recording at 7 points for each ASAD is shown in Figure 6 and the schedule also includes time for replacing batteries. The task distribution and scheduling of the mission are based on the operational sequence of the task. The sequence includes initialization, take-off, flight to the recording point along the planned trajectory, landing, deployment of the sensor, recording the signal, pulling back the sensor, take-off, flight to another recording point or flight back to home position, landing, battery replacement, and mission termination. To ensure that all ASADs record the signal simultaneously, the recording operation must be synchronized. However, significant differences in trajectory lengths can lead to variations in arrival times. The Task List Generator accounts for the longest path, estimates the maximum arrival time, and schedules the recording task for all robots once the last ASAD has landed and deployed its sensor. All the estimated timings of the tasks can be configured by the operator in the FPCS.

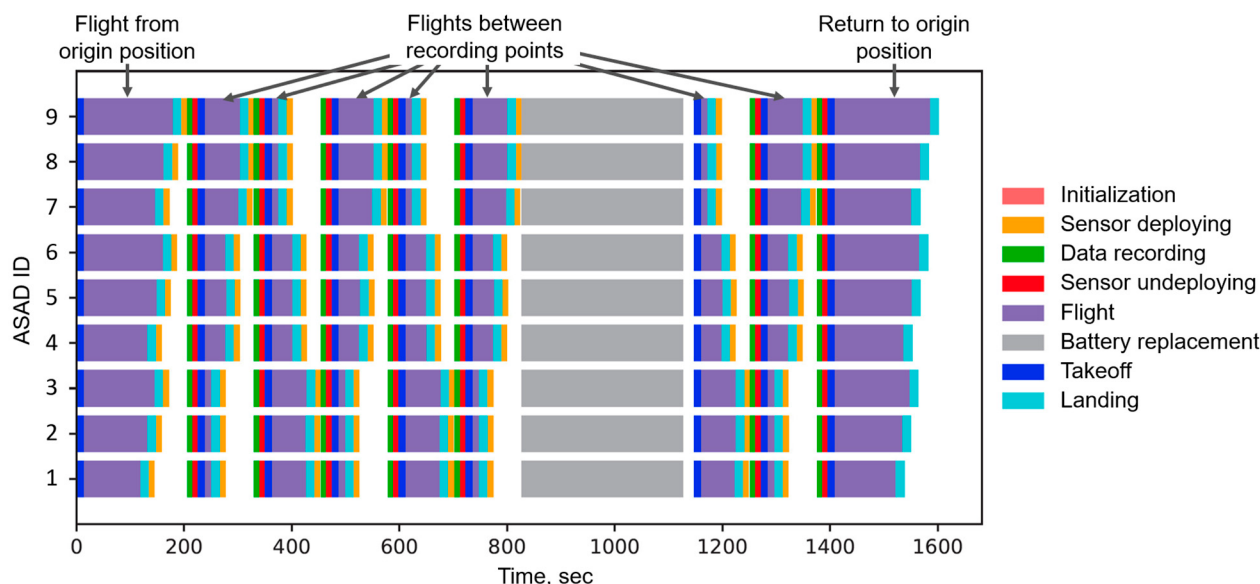


**Figure 6.** Mission schedule of the seismic data acquisition by 9 ASADs.

### 3.3. Selecting an Algorithm for Path Planner

To choose a suitable path-planning algorithm for seismic exploration by ASADs, we implemented and compared APF, A\*, and CHOMP-based algorithms. We considered several factors to evaluate the generated paths, as shown below:

- Average path length;

- Minimum distance between any two paths;
- Calculation time for generating paths.

The analysis was performed for a group of 9 UAVs positioned on a starting grid with 7.5 m between each other. The minimum safe flight distance between UAVs was set at 4.0 m; accordingly, this distance is the minimum distance between any two paths. The straight-line distance of the group to the target positions was 60 m. After conducting calculations and analyzing factors, we concluded that the paths generated by the CHOMP and A\*-based algorithms were superior to those produced using APF. Although the CHOMP required more time for path generation (104.44 s versus 0.56 s for A\*), the minimum distance between trajectories is the closest to the required value, resulting in shorter paths and reduced overall costs. In contrast, the APF-based planner did not prioritize keeping the paths close to each other, resulting in trajectories that were much further apart, leading to longer paths and increased flight time.

The A\* algorithm provides short paths with a faster generation time but maintains a safe distance between trajectories (3.3 m out of 4.0 m). The APF planner requires additional tuning of parameters to generate trajectories similar to those of the CHOMP-based planner. A detailed summary of the experimental outcomes is provided in Table 1. The numbers provided as a result could be proven by visual representation of the generated trajectories, as illustrated in Figure 7. It was decided that the A\* algorithm is a better option for group flights from one recording area to another.

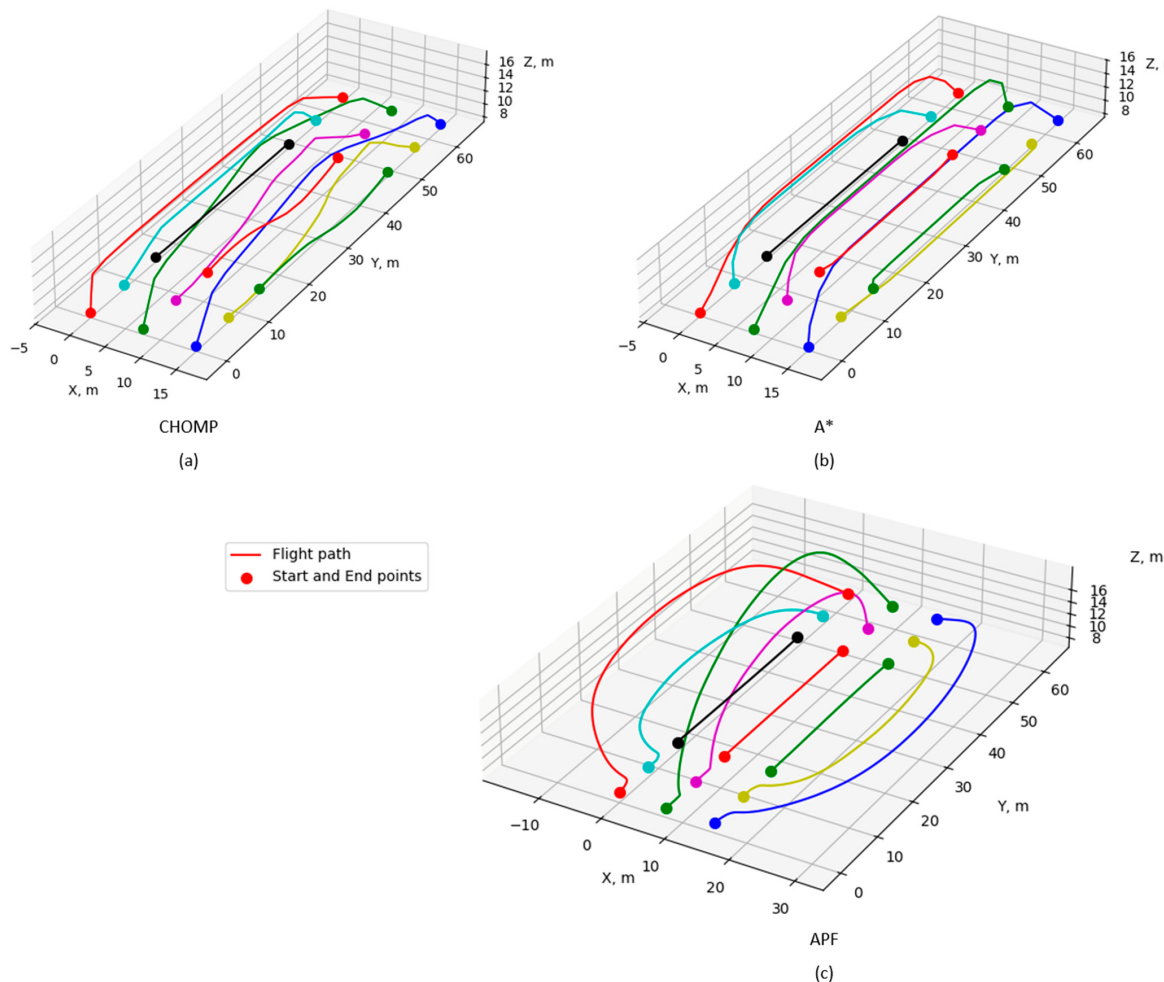


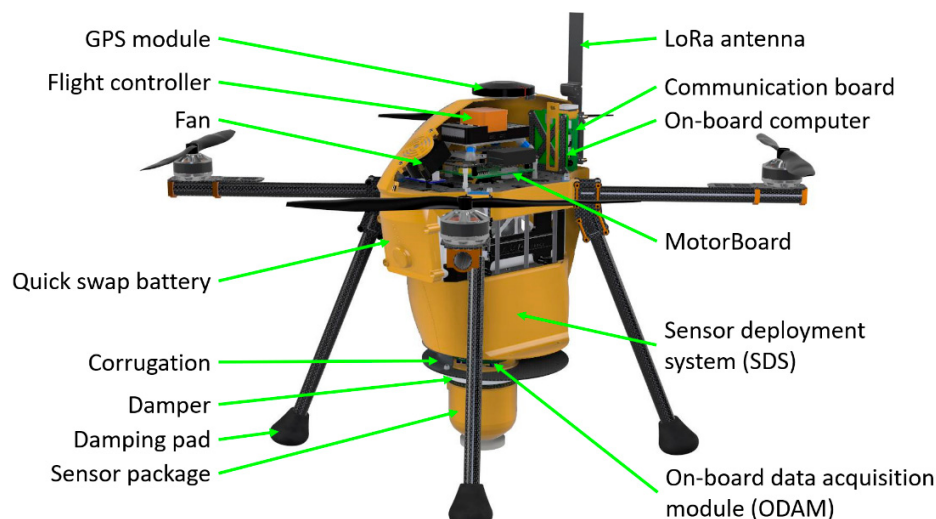
**Figure 7.** Comparison of the trajectories for 9 ASADs, generated by different path-planning algorithms: (a) CHOMP; (b) A\*; (c) APF.

**Table 1.** Path-planning algorithm comparison.

Path-Planning Algorithm	Average Path Length, m	Minimum Distance Between Paths, m	Calculation Time, s
APF based	508.82	3.26	1.76
A*	456.79	3.3	0.56
CHOMP based	456.27	4.03	104.44

### 3.4. The ASAD Layout

The ASAD is a robot consisting of three key functional blocks: a quadrotor platform to navigate and flight, sensor package with three geophones connected to the On-board Data Acquisition Module (ODAM) to record signals and the Sensor Deployment System (SDS) controlled by MotorBoard to provide proper coupling of the sensor package to surface. The blocks are managed by an on-board computer (OBC), which is a single-board computer (Raspberry Pi 4 Model B) with a communication board. The appearance of the ASAD is shown in Figure 8. The block diagram of electronics of ASAD is shown in Figure 9.

**Figure 8.** The layout of ASAD.

The quadrotor platform consists of frames with a diagonal wheel base to equal 665 mm, flight controller (HEX Pixhawk 2.1 CUBE Orange), GNSS (HEX Here 3), RC receiver for remote control, telemetry transceiver, brushless motors and electronic speed controllers (ESCs) for them. The flight controller runs ArduPilot firmware to provide reliable flight control of the robot.

The SDS is a translational mechanism to raise and lower the sensor package, implementing proper coupling to the ground surface. ASAD flies when the sensor package is in a higher position and the SDS is folded. To record signals, the SDS lowers the sensor package and presses it to the ground with the robot's own weight. The DC-motor used in the SDS is controlled by in-house developed MotorBoard. MotorBoard is a printed circuit board, based on a microcontroller unit (MCU) that has an H-bridge integrated circuit (IC) to control the polarity of the voltage for the DC-motor connected.

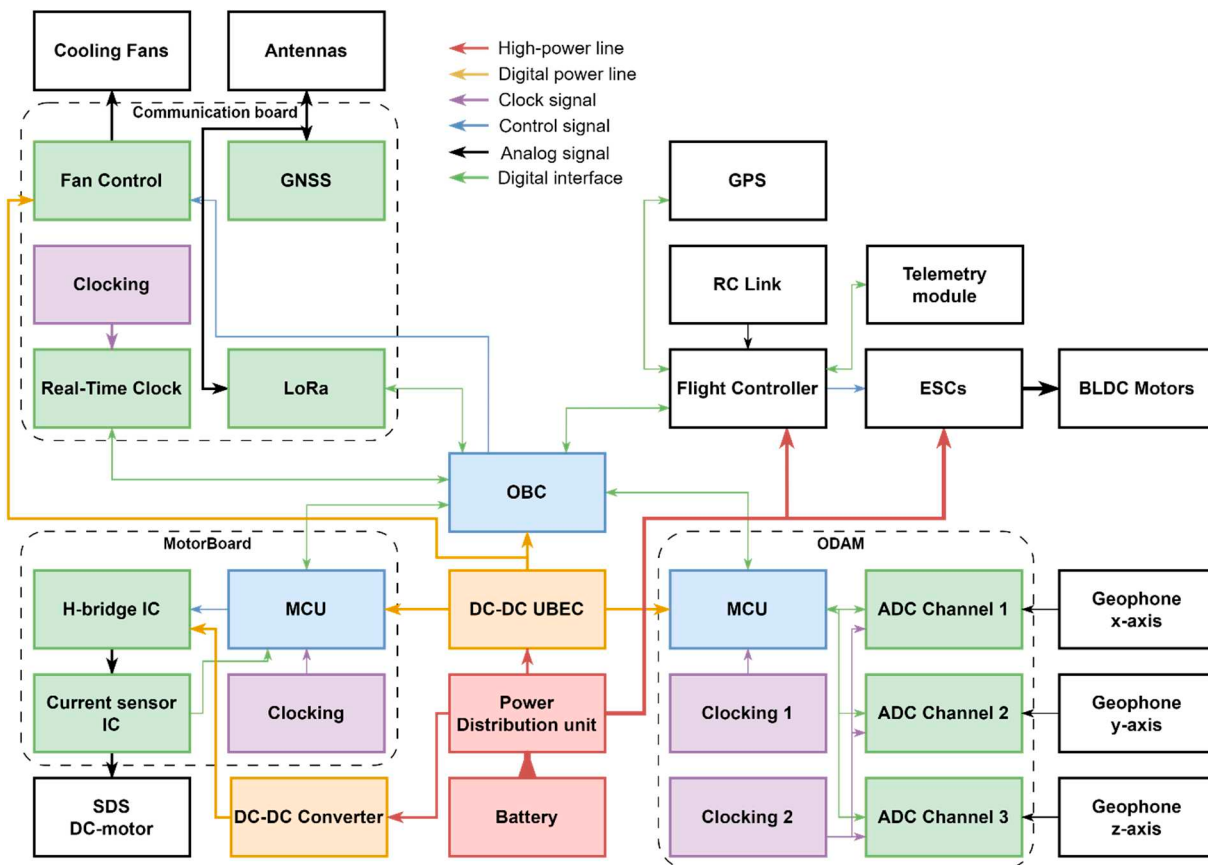


**Figure 9.** The block diagram of the electronics in ASAD.

The sensor package represents three geophones oriented orthogonally along the X, Y and Z axes. These sensors are connected to ODAM. ODAM is an in-house developed electronic board that implements measuring and recording signals from geophones.

The communication board is an additional board with peripheral integrated circuits (ICs) to expand the OBC functionality. It has a real-time clock (RTC), global navigation satellite system (GNSS) module, LoRa module and module to control cooling fans. The MotorBoard and ODAM communicate with OBC through universal serial bus (USB) connection and custom message protocols.

ASAD is powered by a LiPo battery. The power from the battery is distributed among modules by a Power Distribution Module. Then, the voltage is converted to a proper value for components by DC–DC converters. One converter drops the voltage for the SDS motor, and one DC–DC converter with a battery eliminator circuit (BEC) used for digital device power supply.

The current version of the robot is ASAD v.1.3.0. The differences between ASAD versions are presented in Table 2. Modified ASAD has a new dustproof shell with rubber seals in the joints, an updated damper to provide better strength for the SDS, and damping pads to ensure softer landing. ODAM v2.0 is equipped with 32-bit ADCs instead of 24-bit ADCs on ODAM v1.0 to improve the quantization level. The battery is modified by placing it in the quick swap case for quick maintenance.

**Table 2.** ASAD version comparison.

Features	ASAD v.1.1.0 (2022) [1]	ASAD v.1.2.5 (2023) [7]	ASAD v.1.3.0 (2024)
Shell	3D printed (FDM) from PLA	3D printed (SLS) from Nylon (PA-12)	3D printed (SLS) from Nylon (PA-12)
Protection	Basic	Dustproof	IP42
Battery type	Stock	Stock	Quick swap
Legs	2 T-shaped legs (carbon)	4 legs (carbon)	4 legs (carbon) with damping pads (TPE)
SDS	Helical gear	Translational reciprocating–rotational mechanism	Translational reciprocating–rotational mechanism
Damper	v.1.0 (Lasil-V)	v.2.0 (Lasil T-30)	v.2.1 (Lasil T-37)
Tip for sensor package	Metal plate with spikes	Spike, round and triangular plates	Spike, round and triangular plates
Recording system	ODAM v1.0 with external GNSS and RTC modules	ODAM v1.1 with external GNSS and RTC modules	ODAM v2.0
SDS control	H-bridge modules with motor driver TB6612FNG	MotorBoard v.1.0	MotorBoard v.1.1
Cooling system	None	Fan for on-board computer	2 fans

### 3.5. ASAD Control Software

The control software of ASAD is implemented with a robot operating system (ROS). It consists of 5 nodes, which are responsible for interfacing devices and providing some specific function. The nodes are as follows:

- *Communication node* handles the connection with the SCS through the TCP client and LoRa link;
- *Autopilot control node* performs an autonomous mission according to the list of tasks received from the SCS by sending commands to the flight controller, Motorboard and ODAM nodes;
- *Motorboard node* provides communication with the MotorBoard and sends the command for SDS action;
- *ODAM node* provides communication with ODAM, receives and stores the recorded data to the memory and performs the preliminary quality check of the recorded data;
- *Diagnostics node* collects the diagnostics data from all the nodes, forms the diagnostics message for the SCS and sends it through the communication node to the GUI.

A screenshot of the application window with a diagnostics tab for 20 ASADs is shown in Figure 10. In this architecture, the diagnostics node is the node diagnostics collector and decision-making module. Each node has its own diagnostics procedures for self-checking. The communication node is developed to be robust to connection timeouts, messages packet loses, lack of wireless signals, etc. The Motorboard node checks the presence of the MotorBoard among USB devices connected to OBC, and processes potential problems detected by the board MCU. The ODAM node checks the presence of ODAM among USB devices connected to OBC, receives diagnostic information from the MCU of ODAM and can give a command to reset ODAM in case of software problems detected.

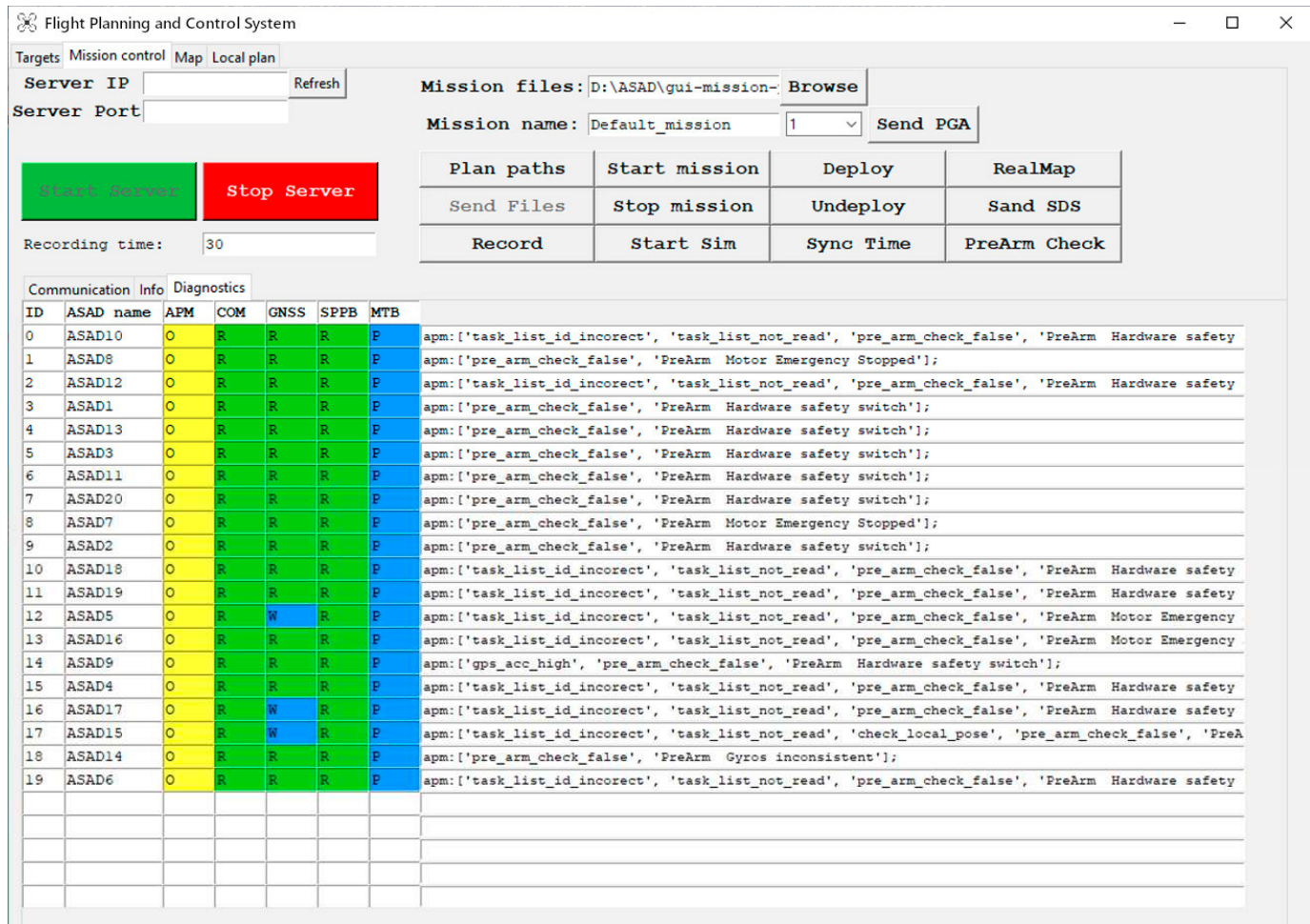


**Figure 10.** The FPCS application diagnostics table for 20 ASADs.

The autopilot control node checks the presence of the flight controller among USB devices connected to OBC, runs MAVROS for data exchange with the flight controller and implements the “preflight check” self-diagnostic procedure. The preflight verifies the readiness of the robot for safe and efficient operation by evaluating a range of parameters and conditions. It begins with an examination of ArduPilot parameter settings, ensuring that essential configurations are properly configured. The procedure validates the correctness of the mission list, confirming that the intended tasks are defined properly. Furthermore, it checks telemetry data, including local position coordinates, battery voltage, and GNSS accuracy. Additionally, pre-arm safety checks are performed to confirm that all prerequisites for flight readiness are completed. The procedure returns a Boolean indicating overall readiness and a list of messages containing any encountered problems, providing the operator with the main information to make informed decisions regarding flight initiation.

The ODAM node is a cyclic script that supports data exchange with the ODAM board via the COM port. The ODAM node provides high-level support for the ODAM board, carrying out the following tasks:

- Sets the main parameters for transmitting measurements—sample rate, signal gain factors, the ADC channel used on the board, etc.;
  - Requests ADC diagnostics for reading errors;
  - Sets the current time set on the OBC;
  - Requests transmission of measurements with the specified parameters for N seconds;
  - Receives and writes measurement data to a file;
  - Performs preliminary processing and quality check of the read data;

- Processes the data acquired by ADCs from ODAM checking for zero-filled data and disproportional noise levels.

### 3.6. Hit Recording Module

The Hit Recording Module (HRM) is a device used to alert the operator of a seismic source and to record a signal near the source to determine the counting time of the emitted wave. A photo of the HRM is shown in Figure 11a. The hardware part consists of the sensor package, power bank, and a Raspberry Pi with LCD display, buzzer, GNSS and LoRa modules. The HRM receives a task list from the SCS, which is similar to the ASAD task list. Also, the SCS sends a command to start the mission through the Wi-Fi module embedded in the on-board computer or through the LoRa.

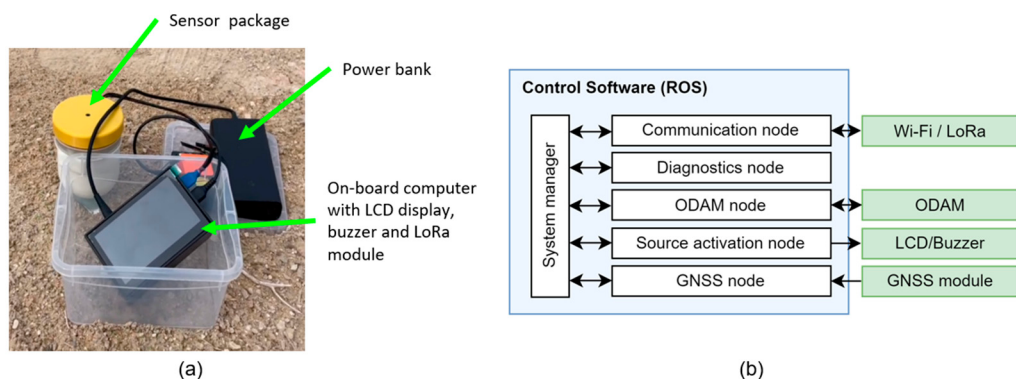


**Figure 11.** Hit Recording Module: (a) photo; (b) software layout of the Hit Recording Module.

After the start of the mission, the countdown begins until the moment when the seismic source should be activated. The HRM software is similar to the ASAD architecture, but it has reduced functionality and consists of 5 nodes (Figure 11b). The communication node is used to receive a task list of the mission, and mission timings. The source activation node is used to inform the operator to activate the seismic source. The GNSS node processes the GNSS data to define the location coordinates for proper data recording. The diagnostics node is used to collect all the local diagnostic data and to transmit it to the SCS through the communication system.

### 3.7. Operating Principal

Before acquisition mission, operator defines a mission scenario of seismic data acquisition using a group of UAVs by setting up the target recording points, source activation points, origin positions and number of available ASADs (Figure 12). ASADs are placed in origin positions in random order at a safe distance from each other with a radius from 3 m. The SCS should be located in the middle of the exploration area to provide reliable communication with ASADs. The Wi-Fi range covers an area with a radius of up to 200 m. The source operator has HRM, which signalizes by sound and message on the display to activate the source. Target points in seismic exploration are numbered from west to east (numbers from 1 to N) and from south to north (numbers from 1 to M). Seismic source activation points are numbered from west to east (numbers from 1 to K). When the system is turned on, ASADs connect to the SCS through Wi-Fi. Then, FPCS distributes target points according to the number of ASADs forming recording areas, in accordance with which the robots will fly cyclically in a rectangular formation until the required area will be completely explored. At the moment, there are two types of missions, as outlined below:

1. Robots follow the source.
2. The source is stationary; robots move away from it.

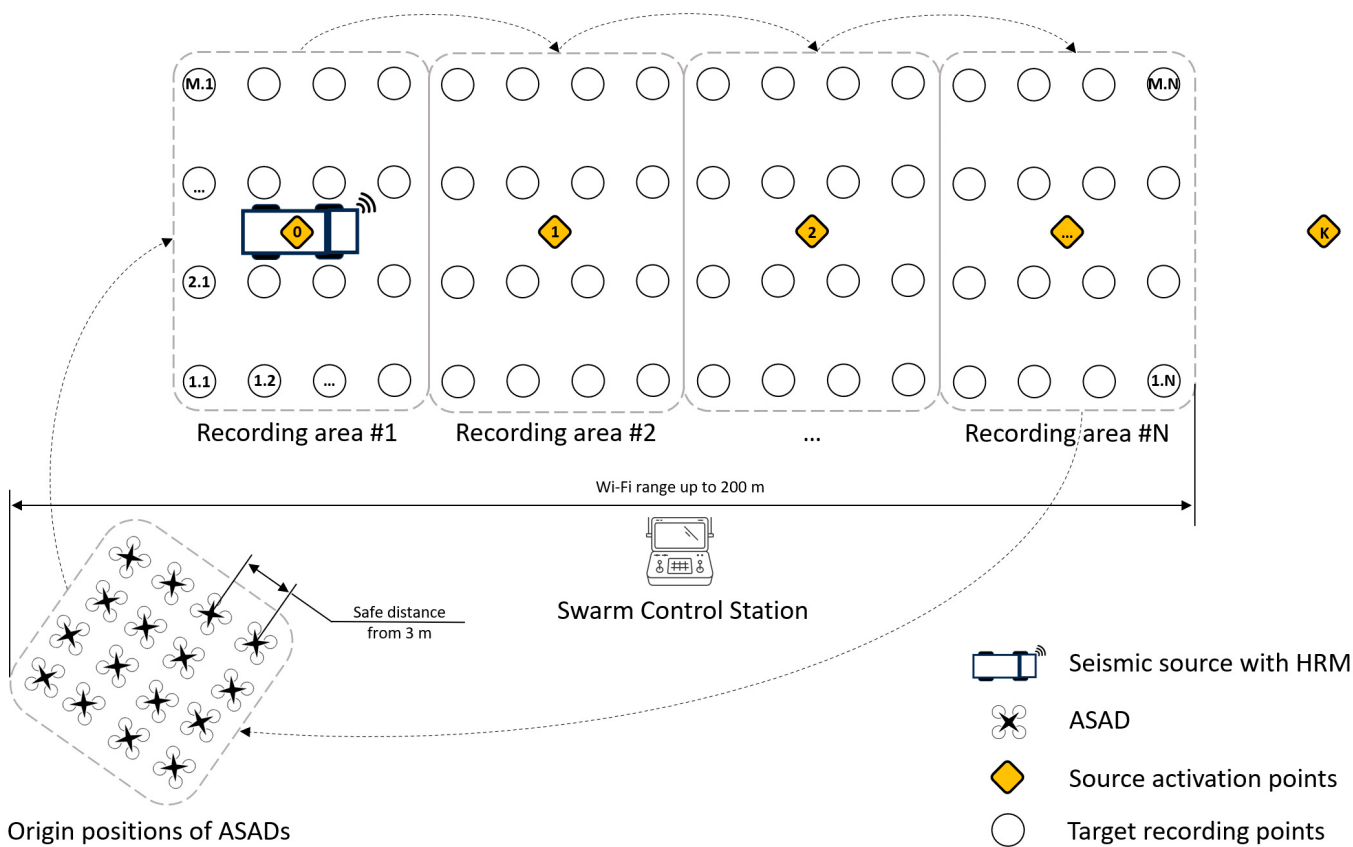


**Figure 12.** General representation of the seismic data acquisition using a group of UAVs.

In both cases, it is necessary to connect the robots to the SCS and set the target points in FPCS. After setting up the mission, FPCS plans flight trajectories, mission task timings and creates task lists for each ASAD. Then, the task lists are sent to its appropriate ASAD and HRM. After this, the operator runs an additional script that connects to the LoRa module on the SCS and sends the current satellite time to the ASADs and HRM to synchronize the system time with the satellite time. The final step before starting the mission is to run the preflight check. For this, the FPCS sends the command to launch this procedure. If the flight controller of any ASAD registered something that may lead to the mission to stop (bad GNSS signal accuracy, inertial measurement unit (IMU) inconsistency), the operator can exclude “sick” ASADs before the start. If all the ASAD’s flight controllers show readiness, the mission may be started. The operator pushes the “Start mission” button on the FPCS and ASADs to start to execute tasks according to the task list. Figure 13 shows the process of how systems’ software blocks interact with each other. Once the UAV swarm mission is started, it performs the seismic survey tasks autonomously, including navigation, data collection, and coordination. However, human supervision is still essential at a high level to monitor the mission’s progress, manage unexpected situations, and ensure safety and battery change.

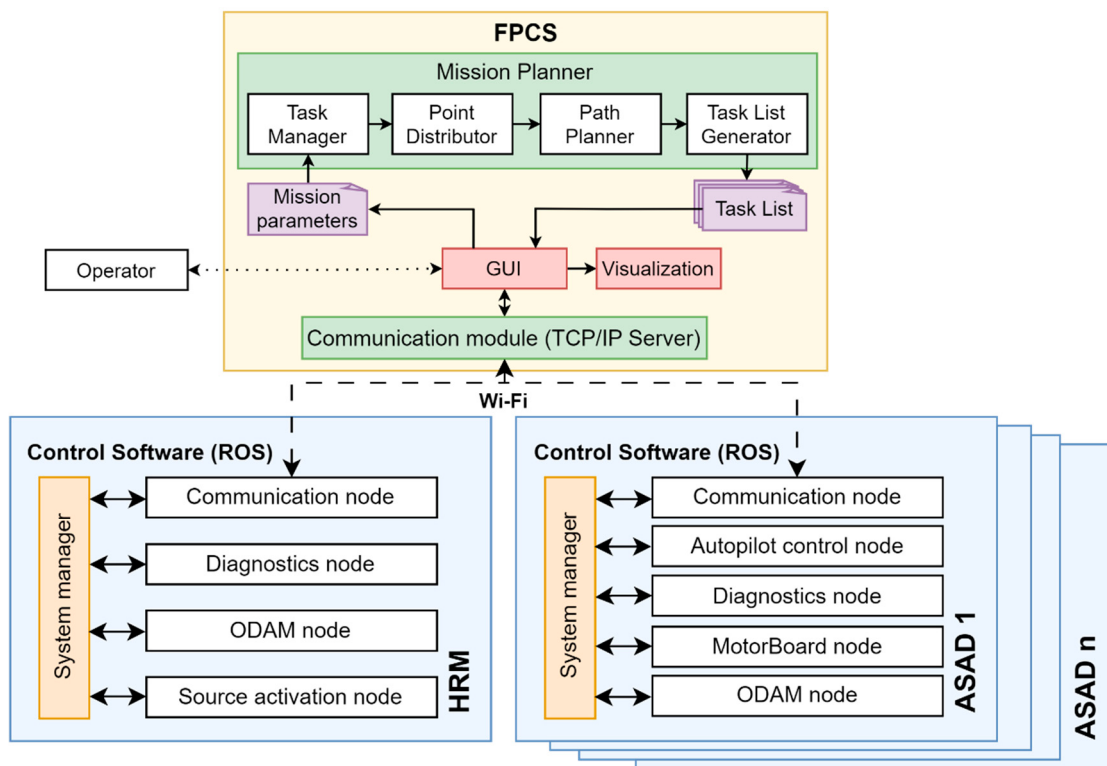


**Figure 13.** Block diagram of the software interaction of the ASAD system.

## 4. Results

### 4.1. Field Test Using 9 ASADs

The following equipment was used: a seismic vibrator as a source of seismic waves, a conventional recording line with 20 recording stations equipped with nine geophones arrays at each station, nine ASADs and SCS. The scheme of the field experiment setup with  $3 \times 3$  ASAD formation is shown in Figure 14. At the first station point, ASADs were placed over a geophone array, each next to the geophone (Figure 15). For recording data at 171 points, the mission was divided into three stages in accordance with the need to change batteries in robots (Figure 16), which leads to the plan of 18 flights for the ASADs to record a signal on a 500 m long trace. The distance between recording areas was 25 m. Nine points near station # 26 were excluded from the flight mission due to the presence of a hill. The sampling rate of the robots was set to 1 msec (1 kHz). Two sweep signals were generated by the seismic vibrator at each recording point for further stacking. The seismic vibrator operator turned on wave emitting after receiving a command from HRM.

Figure 17 shows trace-to-trace comparison for the first test. The data acquired by the ASADs showed results comparable to those obtained with a traditional acquisition system in the form of a recorded wavelet and phase correlation. The best correlation can be observed for the signals recorded by ASADs #1, 5 and 9 that most closely matched the signals registered by geophones located at the same points. The main advantage of utilization of a digital array of nine geophones with subsequent data stacking is to provide data recording at a point of interest even if some of the sensors fail. The same approach was also applied to ASADs, which made it possible to record a signal at the target point even in the case of malfunction of ASAD #6.

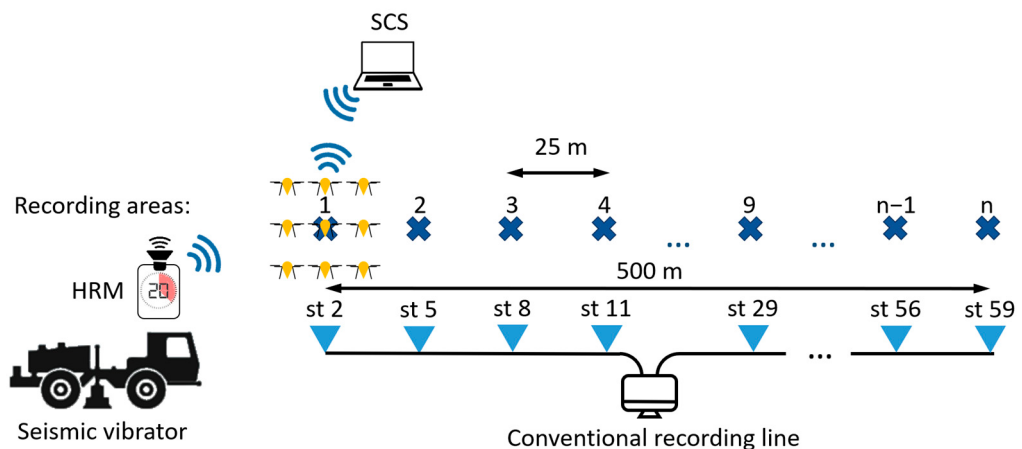


**Figure 14.** Scheme of the field experiment setup with  $3 \times 3$  ASAD formation.

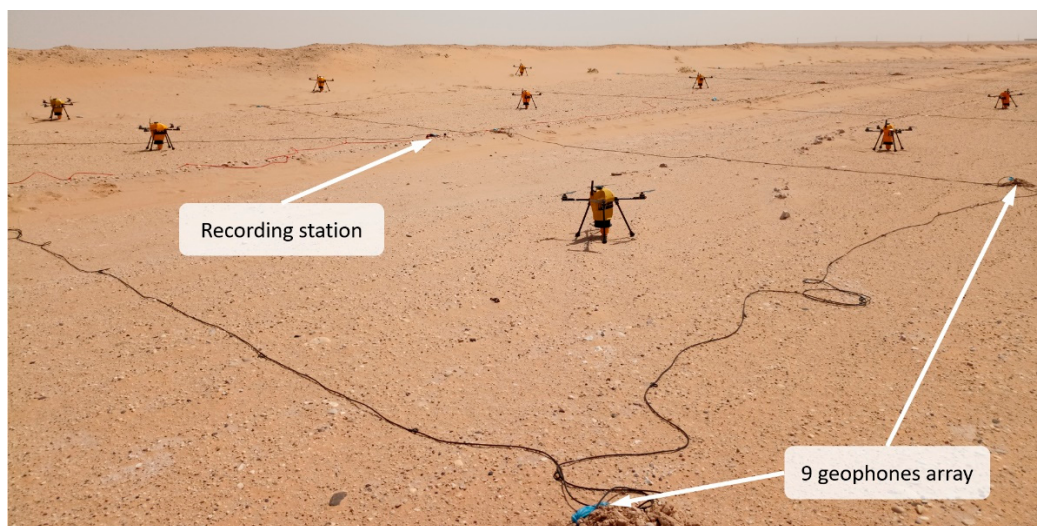


**Figure 15.** Placement of 9 ASADs near station #2 on top of an array of 9 geophones.

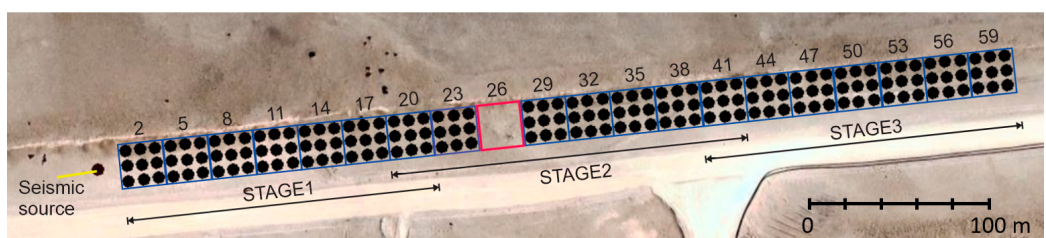


**Figure 16.** Mission pre-plan for test with 9 ASADs.

Comparison of a common shot gather recorded by a nine-geophone array and digital array of nine ASADs is demonstrated in Figure 18. Based on the results, a noticeable difference in the coupling of the conventional system and ASADs can be observed. Up to 200 m, the recorded signal is comparable. The signal is weak but still noticeable at the distance of 200–300 m. After 300 m, the signal is no longer distinguishable against the background noise. This is justified by the fact that conventional geophones were buried properly, while robots were pressing the sensors to the ground surface with their own weight. Nevertheless, the surface wave is the prominent event on the gather recorded by ASADs. The first break can be identified; however, it is already less visible. Amplitude spectra analysis (Figure 19) reveals superior characteristics of the ASAD sensor that was able to record a similar but broader amplitude spectrum than nine-geophone arrays.

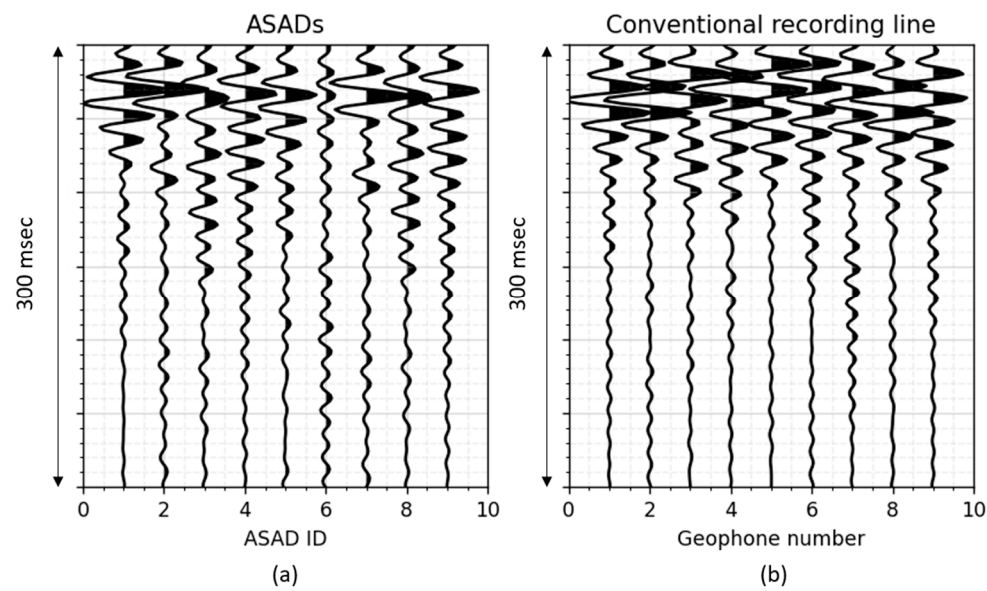


**Figure 17.** Recorded traces at first recording area: (a) array of ASADs and (b) conventional recording line.

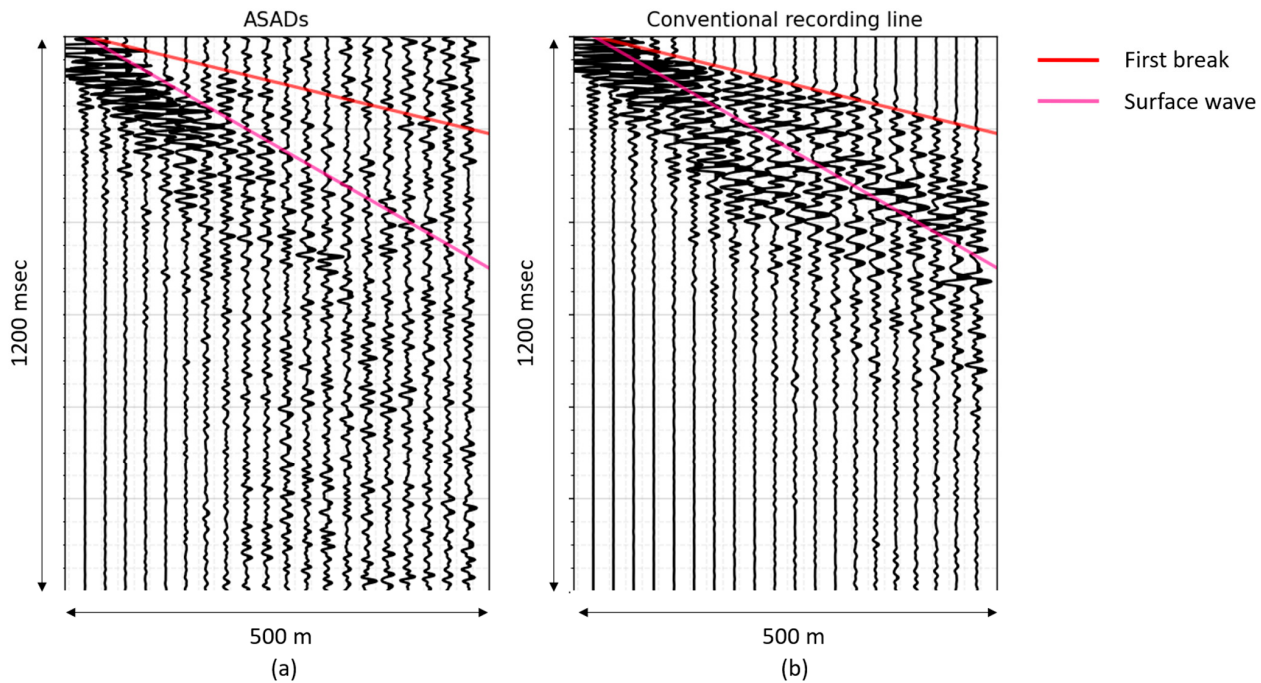


**Figure 18.** Common shot gather recorded by (a) array of ASADs and (b) conventional recording line.

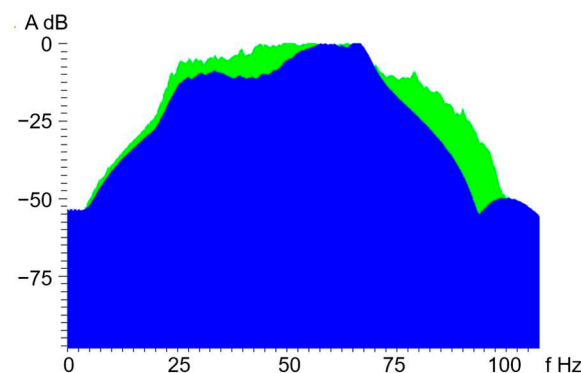


**Figure 19.** Amplitude spectra for ASAD (green) and geophone (blue) traces.

#### 4.2. Field Test Using 16 ASADs

The following equipment was used: a seismic vibrator as a source of seismic waves, 16 ASADs and SCS. The scheme of the field experiment setup with  $4 \times 4$  ASAD formation with 6.25 m spacing is shown in Figure 20. The origin setup for the test is shown in Figure 21. The ASADs shown in the figure are highlighted with their unique identification number in the colored circle. For recording data at 144 points, the mission was divided into two stages in accordance with the need to change batteries in robots (Figure 22), which leads to the plan of eight flights for the ASADs to record a signal on a 243.75 m long trace. The sampling rate on the robots was set to 1 msec (1 kHz). Five sweep signals were generated by a seismic vibrator at nine shot points. The seismic vibrator operator turned on wave emitting after receiving a command from the HRM. The main objective of this experiment was to estimate data quality depending on the surface conditions and sensor to ground coupling. For this, we computed a Signal-to-Noise Ratio (SNR) attribute for each recorded seismic trace. There are many ways to compute the SNR in seismic vibrators; in this case, we took the trace energy ratio of the signal (window 0–500 ms) to noise (window 1000–2500 ms). The SNR attribute map is shown in Figure 23 where one may observe quite significant variations in the recorded data quality depending on the specific UAV as well as surface conditions (the SNR is improving moving east). The GNSS positioning error ranged from 0.47 to 1.87 m (average value was 1.09 m).

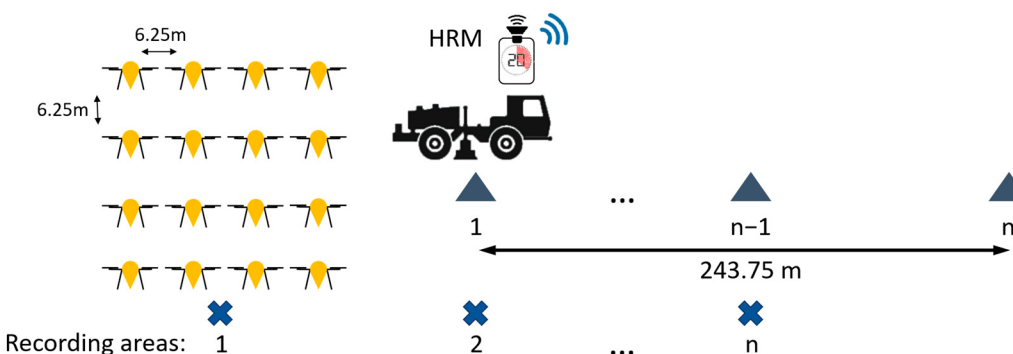


**Figure 20.** Scheme of the field experiment setup with  $4 \times 4$  ASAD formation.

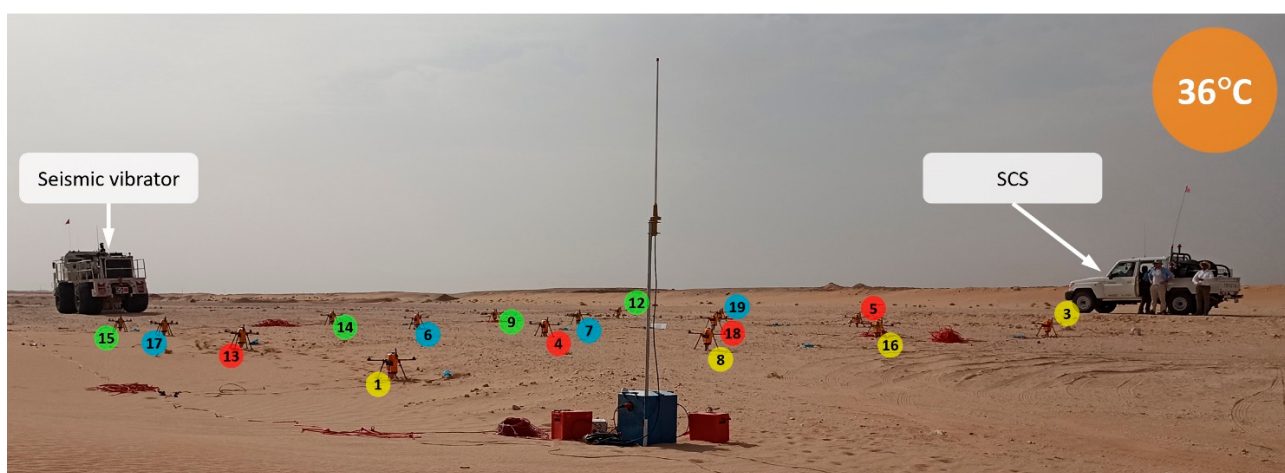


**Figure 21.** Origin setup for test with  $4 \times 4$  ASAD formation.

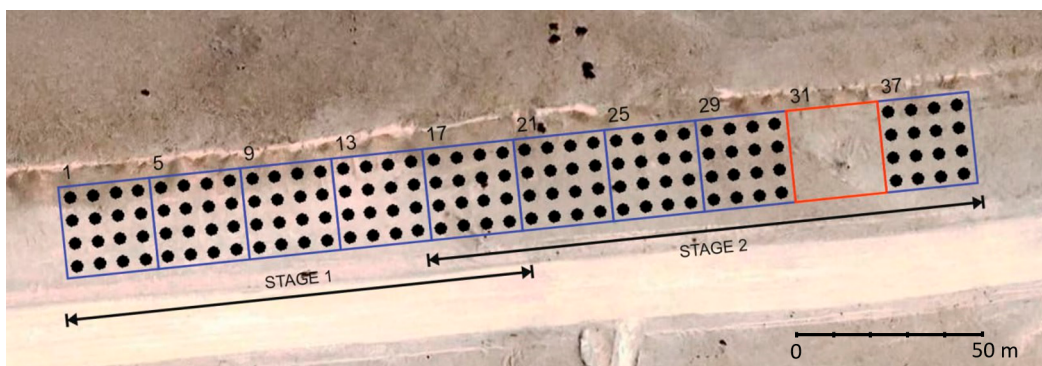


**Figure 22.** Mission preplan for test with 16 ASADs.

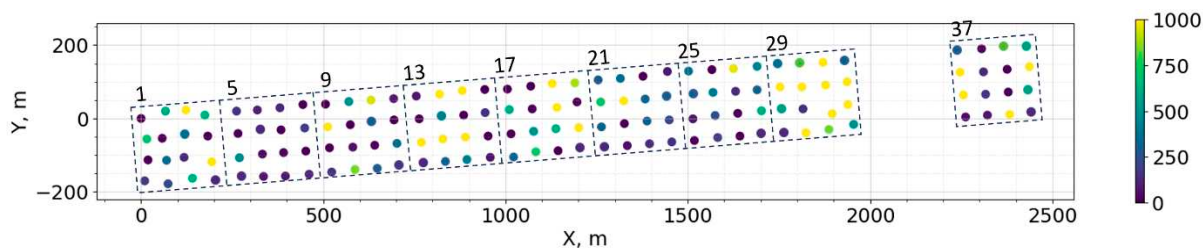


**Figure 23.** SNR attribute computed for the actual recording locations.

## 5. Discussion

A group of ASADs forming an autonomous nodal sensor network with desired survey geometry can enhance the capabilities of a seismic crew. This solution enables efficient coverage of vast areas and can improve safety by minimizing labor work and automating seismic sensor deployment and transportation. With a relatively small number of ASADs, the automated process of deployment using the optimal trajectory strategy and smart swarm management shows promising improvement in productivity in comparison to conventional seismic operation with nodal systems. The developed technology can be used to perform various conventional seismic exploration procedures, such as engineering the survey of ground surfaces before or after the construction of structures, near-surface characterization, acquisition infill, and shallow cavity detection.

Even engineering surveys require a large number of sensors and the developed system must be capable of operating a large number of UAVs. The composition and number of robot groups are determined depending on the limitations of logistics, communication system, and power supply in the field. The ASAD operations can be conducted by several crews, with each crew managing up to 50 or even 100 ASAD units. The swarms can be launched from different areas, and the service crew can move between service points in synchronization with the ASAD swarms' movement. The developed algorithms can also be scaled for larger groups of UAVs with modifications to manage different crews, starting points for UAVs, and services during seismic missions. Also, with an increase in the number of robots, it is necessary to develop the infrastructure for maintenance, including special equipment for battery replacement and charging, development of a reliable communication system over a large area, and the organization of the transportation of robots and related equipment.

Potentially, robust communication of a large group of ASADs may be achieved by using radio with a separate high-altitude UAV for swarm control [40] or using ASAD UAVs as a radio re-translator in the distributed network [41]. These approaches may significantly extend the operation area of the system. The next stage of communication improvement

includes the development of a long-range radio communication system to control the ASAD group over long distances using the SCS.

To upscale the project to an industrial system, it is necessary to perform design improvements, including weight and size characteristic optimization. In addition, ensuring high-quality coupling of the sensor package to the ground surface is one of the main goals for the subsequent modernization of the developed robots. Observations made during the field tests allowed us to identify several reasons for weak SNR: slight swaying of the robot under the influence of the wind and partial pressing of the sensor package to the ground. The swaying is associated with the unstable position of the robot with a lowered sensor package on the uneven surface. The reason for the ASAD swaying and partial pressing of the sensor package may be the heterogeneity of the surface, for example, due to the presence of rocks. Also, pressing the sensor package to a hard surface, such as sandstone, does not ensure a tight fit of the tip to the surface and high-quality signal recording due to the loss of its amplitude. The above problems can be solved by the following improvements: modernization of the SDS mechanism, development of landing gear for aligning the robot on an uneven surface, use of more sensitive seismic sensors (e.g., accelerometers) and/or optimization of the robot design to reduce noise.

Additionally, it is planned to implement obstacle avoidance planning using a map obtained as a result of preliminary aerial photography and to research the optimal swarm navigation patterns to improve operational parameters of the whole ASAD system (system deployment time, data recording time, time required to replace the battery, etc.). The FPCS software can be improved with faster trajectory planning, trajectory optimization, task redistribution in case of malfunction of some robots, and hybrid mission planning in the office and field. Better trajectory quality without compromising computational performance can be potentially achieved by implementation of trajectory smoothing and optimization after A\* path generation.

## 6. Conclusions

Our work focuses on the architecture of a robotic system aimed to perform flexible on-demand seismic exploration targeted at relatively smaller scale but denser data acquisition. The main components of the system are robots named ASADs, which are controlled by FPCS software running on the SCS. At the current development stage, the Wi-Fi network is used for communication between ASADs and the swarm control station. The developed FPCS allows the operator to manage the seismic exploration mission and control the robot actions in a safe manner. Two outdoor tests with 9 and 16 ASAD units were conducted in desert conditions to evaluate the safety of flight control, reliability of sensor coupling, quality of seismic data acquisition, and the optimal level of mission automation. The data acquired by the ODAM embedded in ASADs showed results comparable to the traditional acquisition system in regard to the amplitude, timestamp accuracy and repeatability.

**Author Contributions:** Conceptualization, G.Y., A.T. and P.G.; methodology, A.T., V.S., D.F., G.Y., R.H. and M.K.; software, A.T. and V.S.; validation, A.T., V.S., G.Y., P.G., D.F. and R.H.; formal analysis, G.Y., P.G., A.T. and V.S.; investigation, A.T., G.Y., V.S. and D.F.; resources, P.G. and G.Y.; data curation, A.T., G.Y. and P.G.; writing—original draft preparation, A.T. and G.Y.; writing—review and editing, G.Y., A.T. and P.G.; visualization, G.Y. and A.T.; supervision, G.Y. and P.G.; project administration, P.G. and G.Y.; funding acquisition, P.G. and G.Y. All authors have read and agreed to the published version of the manuscript.

**Funding:** This research received no external funding.

**Data Availability Statement:** Data associated with this research are confidential and cannot be released.

**Conflicts of Interest:** A.T., G.Y., V.S., R.H., D.F. and M.K. were employed by Aramco Innovations LLC, P.G. was employed by EXPEC Advanced Research Center Saudi Aramco. The remaining authors declare that the research was conducted in the absence of any commercial or financial relationships that could be construed as a potential conflict of interest.

## Abbreviations

ADC	Analog-to-digital converter
APF	Artificial potential field
ASAD	Autonomous Seismic Acquisition Device
AUV	Autonomous underwater vehicles
BEC	Battery eliminator circuit
CHOMP	Covariant Hamiltonian Optimization for Motion Planning
CHungSDA	Constrained Hungarian Method for Swarm Drones Assignment
DC	Direct current
DNFOMP	Dynamic Neural Field Optimal Motion Planner
ESC	Electronic speed controller
FPCS	Flight Planning and Control System
GNSS	Global navigation satellite system
GUI	Graphical user interface
HRM	Hit Recording Module
IMU	Inertial measurement unit
LoRa	Long-range radio communication
MAVLink	Micro Air Vehicle Link
MCU	Microcontroller unit
OBC	On-board computer
ODAM	On-board Data Acquisition Module
PF-RRT	Potential field rapidly exploring random tree
ROS	Robotics Operation Systems
RTC	Real-time clock
SCS	Swarm control station
SDS	Sensor Deployment System
SNR	Signal-to-Noise Ratio
TCP	Transmission Control Protocol
UAV	Unmanned aerial vehicle
USB	Universal serial bus

## References

1. Qian, R.; Hu, Y.; Li, P.; Xu, L.; Xiang, Y. Challenges and Solutions for Land Seismic Exploration. In Proceedings of the 2004 SEG Annual Meeting, Denver, CO, USA, 10–15 October 2004; Volume 2024, p. SEG-2004-2545.
2. Golikov, P.; Ramdani, A.; Timoshenko, A.; Yashin, G. Recording Passive Seismic for Shallow Cavities Detection Using an Autonomous Swarm of Seismic Drones. *Eur. Assoc. Geosci. Eng.* **2024**, *2024*, 1–5.
3. Gifford, C.; Agah, A. Robotic Approaches to Seismic Surveying. *J. Autom. Mob. Robot. Intell. Syst.* **2009**, *3*, 13–25.
4. 2023 Summit on Drone Geophysics; Society of Exploration Geophysicists: Houston, TX, USA, 2023.
5. Zheng, Y.; Li, S.; Xing, K.; Zhang, X. Unmanned Aerial Vehicles for Magnetic Surveys: A Review on Platform Selection and Interference Suppression. *Drones* **2021**, *5*, 93. [[CrossRef](#)]
6. Antoine, R.; Lopez, T.; Tanguy, M.; Lissak, C.; Gailler, L.; Labazuy, P.; Fauchard, C. Geoscientists in the Sky: Unmanned Aerial Vehicles Responding to Geohazards. *Surv. Geophys.* **2020**, *41*, 1285–1321. [[CrossRef](#)]
7. Cirillo, D.; Zappa, M.; Tangari, A.C.; Brozzetti, F.; Ietto, F. Rockfall Analysis from UAV-Based Photogrammetry and 3D Models of a Cliff Area. *Drones* **2024**, *8*, 31. [[CrossRef](#)]
8. Thiele, S.T.; Varley, N.; James, M.R. Thermal Photogrammetric Imaging: A New Technique for Monitoring Dome Eruptions. *J. Volcanol. Geotherm. Res.* **2017**, *337*, 140–145. [[CrossRef](#)]
9. Popescu, D.; Ichim, L.; Stoican, F. Unmanned Aerial Vehicle Systems for Remote Estimation of Flooded Areas Based on Complex Image Processing. *Sensors* **2017**, *17*, 446. [[CrossRef](#)] [[PubMed](#)]

10. Cirillo, D. Digital Field Mapping and Drone-Aided Survey for Structural Geological Data Collection and Seismic Hazard Assessment: Case of the 2016 Central Italy Earthquakes. *Appl. Sci.* **2020**, *10*, 5233. [[CrossRef](#)]
11. Ramdani, A.I.; Golikov, P.; Alsoqair, K.; Serpiva, V.; Alfataierge, E. On-Demand High-Resolution Areal Scouting via Unmanned Aerial Vehicles Enables Sustainable near-Surface Geoscience Data Acquisition. *Lead. Edge* **2024**, *43*, 494–505. [[CrossRef](#)]
12. Sudarshan, S.K.V.; Huang, L.; Li, C.; Stewart, R.; Becker, A.T. Seismic Surveying with Drone-Mounted Geophones. In Proceedings of the 2016 IEEE International Conference on Automation Science and Engineering (CASE), Fort Worth, TX, USA, 21–25 August 2016; pp. 1354–1359.
13. Yashin, G.; Serpiva, V.; Timoshenko, A.; Mikhailovskiy, N.; Egorov, A.; Golikov, P. ASAD: Autonomous Seismic Acquisition Device. *Int. J. Control. Autom. Syst.* **2023**, *21*, 2464–2475. [[CrossRef](#)]
14. Sudarshan, S.K.V.; Montano, V.; Nguyen, A.; McClimans, M.; Chang, L.; Stewart, R.R.; Becker, A.T. A Heterogeneous Robotics Team for Large-Scale Seismic Sensing. *IEEE Robot. Autom. Lett.* **2017**, *2*, 1328–1335. [[CrossRef](#)]
15. Khosro Anjom, F.; Browaeys, T.J.; Socco, L.V. Multimodal Surface-Wave Tomography to Obtain S- and P-Wave Velocities Applied to the Recordings of Unmanned Aerial Vehicle Deployed Sensors. *Geophysics* **2021**, *86*, R399–R412. [[CrossRef](#)]
16. Ma, Z.; Qian, R.; Wang, Y.; Zhang, J.; Liu, X.; Ling, J. UAV Source: A New Economical and Environmentally Friendly Source for Seismic Exploration in Complex Areas. *J. Appl. Geophys.* **2022**, *204*, 104719. [[CrossRef](#)]
17. Yashin, G.; Golikov, P.; AlAli, M.N.; Charara, M. System and Method for Seismic Data Acquisition Using Seismic Drones. U.S. Patent US20240230937A1, 11 July 2024.
18. Makama, A.; Kuladinithi, K.; Timm-Giel, A. Wireless Geophone Networks for Land Seismic Data Acquisition: A Survey, Tutorial and Performance Evaluation. *Sensors* **2021**, *21*, 5171. [[CrossRef](#)]
19. Keho, T.H.; Kelamis, P.G. Focus on Land Seismic Technology: The near-Surface Challenge. *Lead. Edge* **2012**, *31*, 62–68. [[CrossRef](#)]
20. Gao, P.; Li, Z.; Li, F.; Li, H.; Yang, Z.; Zhou, W. Design of Distributed Three Component Seismic Data Acquisition System Based on LoRa Wireless Communication Technology. In Proceedings of the 2018 37th Chinese Control Conference (CCC), Wuhan, China, 25–27 July 2018; pp. 10285–10288.
21. Yang, Y.; Chen, Z.B.; Zhang, Y.; Du, Y.J. *Review and Prospect for the Land Seismic Data Acquisition System*; Trans Tech Publications Ltd.: Bäch, Switzerland, 2013; Volume 684, pp. 394–397.
22. Blacquiere, G.; Berkhouit, A.J. *Robotization in Seismic Acquisition*; Schuelke, J., Ed.; SEG: Houston, TX, USA, 2013; pp. 12–16.
23. Dean, T.; Tulett, J.; Barnwell, R. Nodal Land Seismic Acquisition: The next Generation. *First Break* **2018**, *36*, 47–52. [[CrossRef](#)]
24. Tsingas, C.; Kelamis, P.G.; Brizard, T.; Grimsdale, J. Automation in Geophysical Data Acquisition: From Ocean-Bottom Nodes to RoboNodes. *Lead. Edge* **2013**, *32*, 514–520. [[CrossRef](#)]
25. Tsingas, C.; Al Mubarak, M.; Bunting, T. First Wide Scale Field Trial of Autonomous Underwater Vehicles Seismic Programme. In Proceedings of the 82nd EAGE Annual Conference & Exhibition, Amsterdam, The Netherlands, 18–21 October 2021; Volume 2021, pp. 1–5. [[CrossRef](#)]
26. Shin, B.-S.; Patel, D.; Wientgens, L.; Shutin, D.; Dekorsy, A. Multi-Agent 3D Seismic Exploration Using Adapt-Then-Combine Full Waveform Inversion in a Hardware-in-the-Loop System. In Proceedings of the ICASSP 2024—2024 IEEE International Conference on Acoustics, Speech and Signal Processing (ICASSP), Seoul, Republic of Korea, 14–19 April 2024; pp. 12911–12915.
27. Yashin, G.; Mikhailovskiy, N.; Serpiva, V.; Egorov, A.; Golikov, P. Autonomous Flying Robot for the Seismic Exploration. In Proceedings of the 2022 22nd International Conference on Control, Automation and Systems (ICCAS), Jeju, Republic of Korea, 27 November–1 December 2022; pp. 863–868.
28. Boskovic, J.D.; Prasanth, R.; Mehra, R.K. A Multilayer Control Architecture for Unmanned Aerial Vehicles. In Proceedings of the 2002 American Control Conference (IEEE Cat. No.CH37301), Anchorage, AK, USA, 8–10 May 2002; Volume 3, pp. 1825–1830.
29. Zhou, Y.; Rao, B.; Wang, W. UAV Swarm Intelligence: Recent Advances and Future Trends. *IEEE Access* **2020**, *8*, 183856–183878. [[CrossRef](#)]
30. Muliukha, V.; Ilyashenko, A.; Laboshin, L. Network-Centric Supervisory Control System for Mobile Robotic Groups. *Procedia Comput. Sci.* **2017**, *103*, 505–510. [[CrossRef](#)]
31. Tsourdos, A.; White, B.; Shanmugavel, M. *Cooperative Path Planning of Unmanned Aerial Vehicles*; John Wiley & Sons: Hoboken, NJ, USA, 2010.
32. Farid, G.; Cocuzza, S.; Younas, T.; Razzaqi, A.A.; Wattoo, W.A.; Cannella, F.; Mo, H. Modified A-Star (A\*) Approach to Plan the Motion of a Quadrotor UAV in Three-Dimensional Obstacle-Cluttered Environment. *Appl. Sci.* **2022**, *12*, 5791. [[CrossRef](#)]
33. Bentes, C.; Saotome, O. Dynamic Swarm Formation with Potential Fields and A\* Path Planning in 3D Environment. In Proceedings of the 2012 Brazilian Robotics Symposium and Latin American Robotics Symposium, Fortaleza, Brazil, 16–19 October 2012; pp. 74–78.
34. Batinovic, A.; Goricanec, J.; Markovic, L.; Bogdan, S. Path Planning with Potential Field-Based Obstacle Avoidance in a 3D Environment by an Unmanned Aerial Vehicle. In Proceedings of the 2022 International Conference on Unmanned Aircraft Systems (ICUAS), Dubrovnik, Croatia, 21–24 June 2022; pp. 394–401.

35. Huang, T.; Fan, K.; Sun, W.; Li, W.; Guo, H. Potential-Field-RRT: A Path-Planning Algorithm for UAVs Based on Potential-Field-Oriented Greedy Strategy to Extend Random Tree. *Drones* **2023**, *7*, 331. [[CrossRef](#)]
36. Ratliff, N.; Zucker, M.; Bagnell, J.A.; Srinivasa, S. CHOMP: Gradient Optimization Techniques for Efficient Motion Planning. In Proceedings of the 2009 IEEE International Conference on Robotics and Automation, Kobe, Japan, 12–17 May 2009; pp. 489–494.
37. Katerishich, M.; Kurenkov, M.; Karaf, S.; Nenashev, A.; Tsetserukou, D. DNFOMP: Dynamic Neural Field Optimal Motion Planner for Navigation of Autonomous Robots in Cluttered Environment. In Proceedings of the 2023 IEEE International Conference on Systems, Man, and Cybernetics (SMC), Honolulu, HI, USA, 1–4 October 2023; pp. 1984–1989.
38. Nar, D.; Kotecha, R. Optimal Waypoint Assignment for Designing Drone Light Show Formations. *Results Control Optim.* **2022**, *9*, 100174. [[CrossRef](#)]
39. Yong-Fei, M.; Luo, Z.; Luo-Sheng, X. Application of Improved Sparse A\* Algorithm in UAV Path Planning. *Inf. Technol. J.* **2013**, *12*, 4058. [[CrossRef](#)]
40. Xu, C.; Zhang, K.; Jiang, Y.; Niu, S.; Yang, T.; Song, H. Communication Aware UAV Swarm Surveillance Based on Hierarchical Architecture. *Drones* **2021**, *5*, 33. [[CrossRef](#)]
41. Bakirci, M. A Novel Swarm Unmanned Aerial Vehicle System: Incorporating Autonomous Flight, Real-Time Object Detection, and Coordinated Intelligence for Enhanced Performance. *Trait. Signal* **2023**, *40*, 2063–2078. [[CrossRef](#)]

**Disclaimer/Publisher’s Note:** The statements, opinions and data contained in all publications are solely those of the individual author(s) and contributor(s) and not of MDPI and/or the editor(s). MDPI and/or the editor(s) disclaim responsibility for any injury to people or property resulting from any ideas, methods, instructions or products referred to in the content.